Response of lightning NOx emissions and ozone production to climate change: Insights from the Atmospheric Chemistry and Climate Model Intercomparison Project (ACCMIP)

D. L. Finney,[1] R. M. Doherty,[1] O. Wild,[2] P. J. Young,[2] and A. Butler[3]

Corresponding author: D. L. Finney, School of GeoSciences, The University of Edinburgh, Edinburgh, UK (d.finney@ed.ac.uk)

[1]School of GeoSciences, The University of Edinburgh, Edinburgh, UK

[2]Lancaster Environment Centre, Lancaster University, Lancaster, UK

[3]Biomathematics & Statistics Scotland, JCMB, The King's Buildings, Edinburgh, UK

Results from an ensemble of models are used to investigate the response of lightning nitrogen oxide emissions to climate change, and the consequent impacts on ozone production. Most models generate lightning using a parametrization based on cloud-top height. With this approach and a present-day global emission of 5 TgN, we estimate a linear response with respect to changes in global surface temperature of $+0.44 \pm 0.05\,\mathrm{TgN\,K^{-1}}$. However, two models using alternative approaches give $+0.14$ and $-0.55\ \mathrm{TgN\,K^{-1}}$ suggesting that the simulated response is highly dependent on lightning parametrization. Lightning NO_x is found to have an ozone production efficiency of 6.5 ± 4.7 times that of surface NO_x sources. This wide range of efficiencies across models is partly due to the assumed vertical distribution of the lightning source and partly to the treatment of NMVOC chemistry. Careful consideration of the vertical distribution of emissions is needed, given its large influence on ozone production.

1. Introduction

Lightning is the dominant source of nitric oxide in the upper troposphere. In this region of the atmosphere, nitrogen oxides (NO_x) are much more efficient at catalysing ozone production than surface emissions [*Wild*, 2007; *Wu et al.*, 2007; *Dahlmann et al.*, 2011]. Lightning, driven by meteorological conditions, is expected to respond to any future changes in climate. Understanding the sensitivity of this response is important for assessment of future ozone concentrations and associated radiative forcing. In addition, the radiative forcing from methane, which is indirectly influenced by NO_x through reactions with OH, is affected by changes in lightning.

Observational studies suggest that warmer surface temperatures are correlated with increased lightning across diurnal to interannual timescales, although whether such a relationship also applies to longer term climate change remains uncertain [*Williams*, 2005]. Estimates from climate-chemistry models suggest that lightning NO_x emissions will increase by 4-60% per degree increase in global mean surface temperature [*Schumann and Huntrieser*, 2007], with more recent estimates at the lower end of this range [*Zeng et al.*, 2008; *Jiang and Liao*, 2013; *Banerjee et al.*, 2014]. There is a gathering concensus on the sensitivity of lightning NO_x emissions to climate, but this may primarily be due to the similarity of lightning parametrizations used in most models. One isolated study using an alternative lightning parametrization based on ice particle collisions [*Jacobson and Streets*, 2009] found that lightning NO_x emissions decreased as temperatures increased.

The approach used in most global scale models applies a relationship between cloud-top height and lightning [*Price and Rind*, 1992; *Price et al.*, 1997]. This cloud-top height

relationship provides a reasonable proxy for lightning activity but has several limitations. These include a high sensitivity to any biases in modelled cloud-top height and a relatively indirect link to the underlying physical processes [*Tost et al.*, 2007; *Wong et al.*, 2013], which are described by the non-inductive charging theory of storms [*Reynolds et al.*, 1957]. Other parametrizations, related to convection [e.g. *Meijer et al.*, 2001; *Allen and Pickering*, 2002; *Grewe et al.*, 2001; *Romps*, 2014] or cloud ice [e.g. *Deierling et al.*, 2008; *Jacobson and Streets*, 2009; *Finney et al.*, 2014; *Basarab et al.*, 2015], have been demonstrated successfully in individual studies but have yet to be widely adopted. To date there has been little investigation into how these alternative approaches respond to climate change.

The recent Atmospheric Chemistry and Climate Model Intercomparison Project (ACCMIP) provides lightning NO_x emission (LNO_x) distributions from 12 models using three distinct interactive lightning parametrizations under past, present-day and a range of future emission scenarios [*Lamarque et al.*, 2013]. There are 92 relevant multi-year time slice experiments to compare to a multi-year baseline centered around the year 2000 (Table S1), allowing a more complete assessment of lightning sensitivity than has been possible in any previous study. The availability of three distinct parametrizations allows us to explore how the choice of parametrization is important for the emission response to climate change. Ten of the models use the same lightning parametrization based on cloud-top height [*Price and Rind*, 1992], and this allows for the the most rigorous assessment of the climate response of the cloud-top height approach to date. A subset of models, from

which ozone production was archived, is then used to explore how these climate-driven changes in lightning NO_x emissions can influence global ozone production.

2. Statistical Methods

A linear regression assumes independence of data points. However, data produced using the same model share a dependence. To determine robust estimates of the standard errors of regression coefficients when using a multi-model dataset such as in this study, it is appropriate to use a linear mixed effect regression.

Linear mixed effect regressions are extensions of linear regression models which include random effects as well as fixed effects [*Pinheiro and Bates*, 2000; *Bolker et al.*, 2008]. Fixed effects are either numeric or categorical variables for which interest lies in the specific effects of each category. Random effects are categorical variables for which the effects of each category can be regarded as being sampled from a larger population of possible categories, so that interest lies in variation between categories.

In the context of this study, the inclusion of 'model' as a random effect allows for differences in model configuration to be accounted for (through random effects) while estimating the role of explanatory variables (as fixed effects). Both applications of a linear mixed effect regression in this study use a random-slope regression which determines an individual slope and intercept, the random effect, for each model. The random slopes and intercepts are assumed to be correlated.

As with a simple linear regression, it is useful to calculate the variance explained by the regression model, the R^2 value. For linear mixed effect models two values of R^2 can be calculated: the *marginal* R^2, reflecting the proportion of the variance explained by

fixed effects, and the *conditional* R^2, reflecting the variance explained by both fixed and random effects [Supplementary text S1, *Nakagawa and Schielzeth*, 2013; *Johnson*, 2014].

3. Response to Temperature

Generation of thunderstorms is only partly related to the surface temperature, and reflects local rather than global conditions. However, based on past studies, surface temperature provides a simple proxy for changes in the atmosphere that affect lightning.

Figure 1A shows the relationship between total annual lightning NO_x emissions and global mean surface temperature. Each data point is from a single time slice experiment, averaged over multiple years as specified in Table 2 of *Lamarque et al.* [2013], where each year has identical anthropogenic and biomass burning emissions. The data used encompasses time slices of the present-day baseline, historical 1850 and 1980 simulations, and all future scenarios using the Representative Concentration Pathways (RCPs) produced by each model. A significant linear relationship between LNO_x and surface temperature is evident for each model. This is the first time enough comparable data have been produced from a range of models to allow robust conclusions regarding the form of the relationship.

Despite the clear conclusion that each model exhibits a linear relationship, Figure 1A shows a substantial spread between the models. Sources of inter-model spread include the magnitude of the baseline emissions, which vary from 1.3 to 9.7 $\mathrm{TgN\,yr^{-1}}$, and differences in the baseline mean surface temperature which ranges from 286.0 to 288.2 K (see circled points Figure 1A). We remove these variations by normalising the baseline lightning NO_x emissions in each model to 5 TgN and consider changes in temperature and lightning NO_x

emissions relative to this baseline (Figure 1B). The choice of 5 TgN is based on the best estimate for present-day emissions [*Schumann and Huntrieser*, 2007].

Results from models using the cloud-top height approach are grouped together. These models show a consistent linear response of LNO_x to temperature once the differences in present-day surface temperature and global emission totals are adjusted for. A linear mixed effect regression on the data points simulated by models using the cloud-top height approach has been applied. Surface temperature is the regressed fixed effect, while random effects are a random intercept for each model and a random slope for the interaction between each model and the effect of surface temperature. All effects considered are significant at the 5% level and the regression model has a marginal R^2 of 0.82 and a conditional R^2 of 0.96.

A robust estimate of the lightning NO_x emission climate response of $0.44 \pm 0.05\, TgN\, K^{-1}$ is found for models using the cloud-top height approach (individual model fits are provided in Table S2). This corresponds to $8.8 \pm 1.0\%(baseline)\, K^{-1}$, where the uncertainty range represents one standard error. This is lower than the median determined by *Schumann and Huntrieser* [2007] but similar to recent estimates which have a range of 5.5-16 $\% \, K^{-1}$ [Supplementary text S2, *Zeng et al.*, 2008; *Jiang and Liao*, 2013; *Banerjee et al.*, 2014]. Differences in the LNO_x response among models using the cloud-top height approach arise from differing responses to climate change from convective and microphysical schemes, the vertical resolution for resolving cloud-top height and structural differences in implementation of the approach. Details of the lightning parametrization used by each model are described in Supplementary text S3 and Table S3.

The ACCMIP data allow for a robust estimate of the sensitivity of the cloud-top height approach. However, the two ACCMIP models using alternative parametrizations provide rather different estimates. The EMAC model uses a combination of updraft mass flux within the cloud and cloud depth [*Grewe et al.*, 2001] and shows a much weaker sensitivity ($0.14\,\mathrm{TgN\,K^{-1}}$) than the cloud-top approach. The CMAM model uses a parametrization based on updraft mass flux at 440 hPa [*Allen and Pickering*, 2002] and shows the opposite response of a reduction in LNO_x with increasing temperature ($-0.55\,\mathrm{Tg\,K^{-1}}$).

The various responses described above for each parametrization fundamentally depend on the changes in convection simulated by the models. It is possible that these two models are anomalous in their responses to climate change for convection. Further investigation of convection in the different models or application of different parametrizations would be needed to establish this. However, it is unlikely that the models with different lightning parametrizations also have anomalous convection responses and therefore we suggest that the lightning parametrizations are the source of the different responses seen. It is also possible that changes in cloud-top height differ somewhat from changes in the intensity of convective updrafts. *Stevenson et al.* [2005] and *Banerjee et al.* [2014] have found that in some locations the occurrence of deep convection decreases under climate change but that the depth increases. Our findings suggest that it is vital to determine whether the cloud-top height approach provides the most appropriate representation of lightning, or whether a greater diversity of lightning parametrizations is needed. Uncertainty remains as to whether lightning NO_x emissions will increase or decrease in future.

4. Spatial Variation of Response to Temperature

The impacts of LNO_x on atmospheric chemistry and radiative forcing are dependent on the spatial distribution of emissions as well as the global total [*Liaskos et al.*, 2015; *Finney et al.*, 2016]. We consider here the spatial distribution of LNO_x and change in LNO_x between present-day and future, and whether there is anomalous behaviour underlying the distributions.

Figure 2A-C shows the mean baseline (year 2000) distribution of lightning NO_x emissions from eight models using the cloud-top height approach for which spatial distributions of emissions are available, as well as from each of the models using alternative schemes. The emission distributions of all three approaches represent, to a reasonable extent, the climatological distribution of lightning flash rate provided by the Lightning Imaging Sensor and Optical Transient Detector [*Cecil et al.*, 2012]. In particular, they show lightning NO_x emission peaks in tropical continental locations, and lower values towards the poles and over the oceans. The distributions of change in surface temperature (Figure S4) and precipitation (Figure S5) between the present-day and year 2100 using the RCP8.5 scenario are shown in supplementary material. CMAM and EMAC do not simulate anomalous temperature or precipitation changes compared to the other ACCMIP models. The robustness of these two models, which use alternative lightning parametrizations, among the other ACCMIP models regarding these three variables gives confidence that they are not outliers in terms of their broad representation of climate change.

Figures 2D-F show the absolute changes in lightning NO_x emissions between the present-day and year 2100 using the RCP8.5 scenario for each type of lightning parametrization.

As with the global total LNO_x changes in Figure 1, the three approaches represent largely positive (Figure 2D), mixed (Figure 2E) and largely negative changes (Figure 2F). From all three approaches, it is clear that changes in LNO_x under future climate change are non-uniform. The largest absolute changes typically occur where there are highest baseline lightning NO_x emissions and the sign of these changes are generally consistent with the sign of global total LNO_x changes found with each lightning parametrization.

The percentage changes in lightning NO_x emissions between the present-day and year 2100 using the RCP8.5 scenario are shown in Figures 2G-I. The changes in the models using alternative schemes appear more noisy. This is partly due to averaging over a number of models that use CTH (Figure 2G), but even compared to individual model simulations of LNO_x based on cloud-top height the alternative schemes produce a more heterogeneous response (Figure S3). The cloud-top height will be partly limited by the tropopause which will vary smoothly and, therefore, may lead to smoothness in the simulated LNO_x distribution by models using the CTH approach.

Percentage changes between present-day and future are generally large over ocean as well as over land. Most of the globe experiences changes of >10%. While absolute changes in LNO_x are small away from dominant source regions, the percentage changes are larger away from high emission regions. Such large relative changes may be important in remote locations where there are few other sources of NO_x.

There is agreement between the different schemes on the sign of the change in some locations which can be seen in Figure 2 G-I. Mostly these are located in the mid-latitudes. Increases in LNO_x in the Northeast Atlantic and Pacific suggest an increase in lightning

activity within northern mid-latitude storms or a shift in location of the storm tracks. Decreases in the Southeast Pacific are consistent with significant drying reported in the IPCC AR5 report by *Collins et al.* [2013, Fig. 12.22]. *Collins et al.* [2013] indicated significantly increased rainfall in Russia and eastern Canada in year 2100 under RCP8.5, corresponding to increases in LNO_x in Figures 2 G-I, thereby suggesting the changes in rainfall in these regions correspond to changes in the frequency or intensity of thunderstorms. There are many other locations where changes in lightning NO_x emissions do not correspond to similar changes in precipitation. The non-uniformity of these changes in lightning is an important argument for using interactive lightning schemes that are not constrained spatially by present-day observations.

5. Ozone Production

Ozone production is sensitive to a large number of variables influenced by climate change and so it is difficult to attribute changes in ozone concentration directly to changes in lightning NO_x emissions. Changes in temperature, humidity, deposition, other ozone precursor emissions and stratosphere-troposphere exchange all contribute to changes in ozone [*Fiore et al.*, 2012; *Doherty et al.*, 2013; *Young et al.*, 2013]. The most direct impact of lightning NO_x emissions on ozone is through chemical production.. Based on model sensitivity studies, *Wild* [2007] found that an increase in LNO_x produced ~ 3 times more global tropospheric ozone production per Tg(N) than an increase in surface NO_x emissions. Using alternative methods, *Wu et al.* [2007] and *Dahlmann et al.* [2011] found that LNO_x produced six and five times more ozone that surface NO_x, respectively. This disproportionately large effect is due to lightning NO_x emission in the middle and upper

troposphere where temperatures are cooler, NO_x and ozone have longer lifetimes, and where ozone production efficiency is high.

Tropospheric ozone chemical production fluxes were archived from a subset of six models during ACCMIP. Relevant emission variables from all time slices and scenarios (Table S1) are used here to perform a linear mixed effect regression to describe global tropospheric ozone production. Fixed effects for lightning NO_x, surface NO_x, CO and NMVOC emissions and the methane tropospheric burden were included within the initial mixed effect regression, along with random effects for 'model' and for the interaction between 'model' and the effect of lightning. The surface NO_x variable includes NO_x emissions from aircraft but these are less than 2% of the total emissions and we assume that their effects are small.

A stepwise selection process, based on the Akaike information criteria (AIC) [*Burnham and Anderson*, 2002], was used to identify whether the initial regression model could be simplified, and this led to NMVOC emissions and CO emissions being removed. The remaining explanatory variables all have significant coefficients with $p < 0.05$. The model has a *marginal* R^2 of 0.57 and a *conditional* R^2 of 0.99. An equation for the fitted linear model is given by:

$$\hat{P} = 104(\pm 37)E_{LNO_x} + 16.0(\pm 0.9)E_{surfNO_x} + 0.0793(\pm 0.0104)B_{CH_4} - 1.85(\pm 14.74) + U_{1,m}E_{LNO_x} + U_{2,m} \quad (1)$$

where $\hat{P}$ is the estimated global tropospheric ozone production ($\mathrm{mol}(O_3)\mathrm{yr}^{-1}$), E_{LNO_x} and E_{surfNO_x} are emissions of lightning NO_x and surface NO_x ($\mathrm{mol(N)yr}^{-1}$), and B_{CH_4} is methane tropospheric burden ($\mathrm{mol}(CH_4)$). Ranges given in Equation 1 are the stan-

dard errors associated with each coefficient. The random model slope, $U_{1,m}$, represents an adjustment to the fixed lightning effect, and the random model intercept, $U_{2,m}$, an adjustment to the regressed intercept, for each model, m. There are six models and therefore U_1 and U_2 are each a vector of six values. The mean of the values of any random effect, U, is zero. The standard deviations of the values of $U_{1,m}$ and $U_{2,m}$ are 75 and 28, respectively.

The coefficients of Equation 1 represent the number of moles of ozone produced for each mole of the species, i.e., the ozone production efficiency (OPE). For example, the OPE associated with surface NO_x sources is 16 $\mathrm{mol}(O_3)\,\mathrm{mol}^{-1}(\mathrm{N})$. The underlying fixed LNO_x effect found in the regression is 6.5 times larger than that of surface NO_x sources, similar to that found by *Wu et al.* [2007] and *Dahlmann et al.* [2011], and representing a disproportionally larger efficiency of LNO_x in producing ozone.

It is important to consider the size of the emissions or burden in combination with regression coefficients to fully understand the context of the statistical regression results. By applying the regressed ozone production efficiencies of Equation 1 for E_{LNO_x} including the random slopes, E_{surfNO_x}, and B_{CH_4} to the emissions in each time slice experiment we can attribute a proportion of the estimated ozone production to each of the individual effects. There are 50 time slice experiments used (summarized in Table S1). The mean and range for the three effects is: $E_{LNO_x}41\%(3-78\%)$, $E_{surfNO_x}38\%(12-68\%)$ and $B_{CH_4}21\%(9-51\%)$. These results show that the three effects, at least for the range of experiments in ACCMIP, produce similar amounts of ozone, with CH_4 generally producing less ozone and with a wider range of contributions to ozone production from LNO_x across the experiments.

6. Causes of Variability in Ozone Production Efficiency

The regression model described by Equation 1 provides a means to remove the estimated ozone production by species other than LNO_x and therefore study the production by LNO_x alone. In addition the random slope values, $U_{1,m}$, determined in the regression can either be removed to see the estimated underlying ozone production from LNO_x across models, or included to see the estimated ozone production from LNO_x in each model. These components of ozone production are shown by the partial residuals of ozone production against LNO_x in Figures 3A and B.

The partial residual is the actual ozone production with the estimated ozone production of some terms in the regression removed. Figure 3A is the conditional partial residual of ozone production with respect to lightning NO_x emissions, ϵ_1, i.e., the general relationship across models given by the fixed effect of E_{LNO_x} in Equation 1 and described by Equation 2:

$$\epsilon_1 = \hat{P} - 16.0E_{surfNO_x} - 0.0793B_{CH_4} - 1.85 - U_{1,m}E_{LNO_x} - U_{2,m} \quad (2)$$

Figure 3B shows the individual model relationships between ozone production and LNO_x, ϵ_2, i.e., the combination of the fixed effect, E_{LNO_x}, and individual random slopes, $U_{1,m}$. This partial residual residual is described by Equation 3:

$$\epsilon_2 = \hat{P} - 16.0E_{surfNO_x} - 0.0793B_{CH_4} - 1.85 - U_{2,m} \quad (3)$$

These partial residuals demonstrate the effect of lightning NO_x emissions and clearly reveal the differences in OPE between the models.

The vertical distribution of LNO_x differs greatly between the models, as shown in Figure 3C. Vertical distribution methods are based upon modelled updrafts, prescribed distribu-

tions [*Pickering et al.*, 1998; *Ott et al.*, 2010], or air density [*Goldenbaum and Dickerson*, 1993; *Stockwell et al.*, 1999; *Jourdain and Hauglustaine*, 2001]. The LNO_x vertical distribution method used by each model in ACCMIP is given in Table S3.

The proportion of lightning NO_x emission in the middle and upper troposphere (500-100 hPa) and the gradient (OPE) for each individual model determined by the mixed effect regression are presented in Figure 3B. Although there are relatively few models, there is a direct relationship between the amount of ozone in the middle and upper troposphere and the OPE of lightning. An exception is the CMAM model which has a relatively weak relationship between ozone production and LNO_x and a low OPE. It would require a targeted study to identify the cause of this difference, but we note that CMAM does not include NMVOC chemistry, representing this instead through extra CO emissions. The majority of NMVOC emissions are in the form of biogenic emissions and are high over tropical rainforests where lightning activity is also high. It is possible that the combined emissions of NMVOC and LNO_x increase OPE in these regions through a greater radical pool. CMAM also has a different spatial distribution of the response of LNO_x to climate change compared to other models. Changes in regions of lower ozone production may contribute to a weaker relationship between ozone production and LNO_x.

The considerations above encourage further research to understand variability among models. LNO_x and OPE will have seasonal and regional responses to climate change which have not been investigated here. Furthermore, research into the effect on OPE of LNO_x being concentrated within convective outflow plumes would be valuable, given that this feature is not captured by the resolutions of ACCMIP models. Dedicated sensitivity

simulations within a climate-chemistry model would allow quantification of the role of the vertical emission distribution of lightning NO_x and the representation of NMVOCs on the OPE of LNO_x. This would permit these effects to be isolated and allow determination of the contribution of LNO_x differences to the inter-model variation of OPE in Figure 3B. The standard deviation of individual model estimates of OPE can be used as a proxy for the uncertainty on the fixed LNO_x effect discussed in Section 5, suggesting that the OPE of LNO_x is 6.5 $\pm$ 4.7 times that of surface NO_x sources.

7. Conclusions

The large dataset of model results archived for ACCMIP has allowed a rigorous analysis of the climate sensitivity of lightning NO_x emissions for models using the cloud-top height parametrization of *Price and Rind* [1992]. This parametrization is widely used and performs very similarly across models with a positive linear response of $0.44 \pm 0.05\, TgN\, K^{-1}$ for a baseline annual emission of 5 TgN. Two models using different parametrizations of lightning simulate a weaker and an opposite climate response of lightning NO_x emissions. Therefore, despite the important role that lightning NO_x emission plays in ozone chemistry, it is clear from the two ACCMIP models using alternative lightning schemes that there cannot be complete confidence in the magnitude or even sign of the lightning NO_x emission sensitivity to climate change. While there is agreement among the three parametrizations in a few locations regarding the projected spatial change of LNO_x in future, generally this is as uncertain as the global changes.

There is no indication that the models using alternative schemes are outliers in terms of their representation of surface temperature or precipitation change. We therefore conclude

that the different responses of lightning to climate change are due to the use of different lightning parametrizations. Studies establishing the climate sensitivity of multiple lightning parametrizations within the same model are needed to confirm whether the results here solely reflect the different parametrizations. The cloud-top height approach has been well characterised in this study thereby providing a useful reference point in understanding the behaviour of alternative schemes. We therefore suggest that climate-chemistry modelling groups consider additional simulations with alternative lightning schemes, as a greater diversity of schemes would help advance our understanding of uncertainties in the response of lightning NO_x to climate change and its subsequent effects on ozone.

Uncertainty in the climate response of lightning will undoubtedly lead to uncertainty in the changes in ozone production from LNO_x. The tropospheric ozone production from LNO_x and other sources has been quantified using the data from a selection of models in ACCMIP. The results suggest that lightning NO_x emissions are 6.5 ± 4.7 times more efficient than surface NO_x sources at producing ozone in the troposphere. The method for distributing emissions vertically as well as the treatment of emissions of NMVOCs appear to be responsible for at least some of this variability in ozone production efficiency from lightning. Therefore, direct determination of the role of the vertical LNO_x distribution for ozone production is necessary before a consistent approach among models can be developed.

Acknowledgments. Declan Finney was supported by a Natural Environment Research Council grant NE/K500835/1. Adam Butler's contribution was supported by the Rural and Environment Science and Analytical Services (RESAS) Division of the Scot-

tish Government. We thank model groups contributing to ACCMIP for use of their data, in particular, David Plummer for discussions regarding CMAM. Access to the ACCMIP dataset can be requested from the British Atmospheric Data Centre. We are grateful to Oliver Binks and Claudia Steadman for discussions regarding mixed effects models.

References

Allen, D. J., and K. E. Pickering (2002), Evaluation of lightning flash rate parameterizations for use in a global chemical transport model, *J. Geophys. Res.*, *107*(D23), 4711, doi:10.1029/2002JD002066.

Banerjee, A., A. T. Archibald, A. C. Maycock, P. Telford, N. L. Abraham, X. Yang, P. Braesicke, and J. A. Pyle (2014), Lightning NOx, a key chemistry-climate interaction: Impacts of future climate change and consequences for tropospheric oxidising capacity, *Atmos. Chem. Phys.*, *14*, 9871–9881, doi:10.5194/acp-14-9871-2014.

Basarab, B. M., S. A. Rutledge, and B. R. Fuchs (2015), An improved lightning flash rate parameterization developed from Colorado DC3 thunderstorm data for use in cloud-resolving chemical transport models, *J. Geophys. Res.*, *120*, doi: doi:10.1002/2015JD023470.

Bolker, B. M., M. E. Brooks, C. J. Clark, S. W. Geange, J. R. Poulsen, M. H. H. Stevens, and J.-S. S. White (2008), Generalized linear mixed models: A practical guide for ecology and evolution, *Trends Ecol. Evol.*, *24*(3), 127–135, doi:10.1016/j.tree.2008.10.008.

Burnham, K. P., and D. R. Anderson (2002), *Model selection and multimodel inference: A practical information-theoretic approach*, Springer.

Cecil, D. J., D. E. Buechler, and R. J. Blakeslee (2012), Gridded lightning climatology from TRMM-LIS and OTD: Dataset description, *Atmos. Res.*, *135-136*, 404–414, doi: 10.1016/j.atmosres.2012.06.028.

Collins, M., R. Knutti, J. Arblaster, J.-L. Dufresne, T. Fichefet, P. Friedlingstein, X. Gao, W. J. Gutowski, T. Johns, G. Krinner, M. Shongwe, C. Tebaldi, A. J. Weaver, and M. Wehner (2013), Long-term climate change: Projections, commitments and irreversibility, *Climate Change 2013: The Physical Science Basis. Contribution of Working Group I to the Fifth Assessment Report of the Intergovernmental Panel on Climate Change [Stocker, T. F., D. Qin, G.-K. Plattner, M. Tignor, S. K. Allen, J. Boschung, A. Nauels, Y. Xi]*, pp. 1029–1136, doi:10.1017/CBO9781107415324.024.

Dahlmann, K., V. Grewe, M. Ponater, and S. Matthes (2011), Quantifying the contributions of individual NOx sources to the trend in ozone radiative forcing, *Atmos. Environ.*, *45*(17), 2860–2868, doi:10.1016/j.atmosenv.2011.02.071.

Deierling, W., W. A. Petersen, J. Latham, S. Ellis, and H. J. Christian (2008), The relationship between lightning activity and ice fluxes in thunderstorms, *J. Geophys. Res.*, *113*, D15,210, doi:10.1029/2007JD009700.

Doherty, R. M., O. Wild, D. T. Shindell, G. Zeng, I. A. MacKenzie, W. J. Collins, A. M. Fiore, D. S. Stevenson, F. J. Dentener, M. G. Schultz, P. Hess, R. G. Derwent, and T. J. Keating (2013), Impacts of climate change on surface ozone and intercontinental ozone pollution: A multi-model study, *J. Geophys. Res. Atmos.*, *118*, 1–20, doi:10.1002/jgrd.50266.

Finney, D. L., R. M. Doherty, O. Wild, H. Huntrieser, H. C. Pumphrey, and A. M. Blyth (2014), Using cloud ice flux to parametrise large-scale lightning, *Atmos. Chem. Phys.*, *14*(12), 12,665–12,682, doi:10.5194/acp-14-12665-2014.

Finney, D. L., R. M. Doherty, O. Wild, and N. L. Abraham (2016), The impact of lightning on tropospheric ozone chemistry using a new global parametrisation, *Atmos. Chem. Phys. Discuss.*, doi:10.5194/acp-2016-59, in review.

Fiore, A. M., V. Naik, D. V. Spracklen, A. Steiner, N. Unger, M. Prather, D. Bergmann, P. J. Cameron-Smith, I. Cionni, W. J. Collins, S. Dalsøren, V. Eyring, G. a. Folberth, P. Ginoux, L. W. Horowitz, B. Josse, J.-F. Lamarque, I. A. MacKenzie, T. Nagashima, F. M. O'Connor, M. Righi, S. T. Rumbold, D. T. Shindell, R. B. Skeie, K. Sudo, S. Szopa, T. Takemura, and G. Zeng (2012), Global air quality and climate, *Chem. Soc. Rev.*, *41*(19), 6663–6683, doi:10.1039/c2cs35095e.

Goldenbaum, G. C., and R. R. Dickerson (1993), Nitric oxide production by lightning discharges, *J. Geophys. Res.*, *98*(D10), 18,333–18,338.

Grewe, V., D. Brunner, M. Dameris, J. Grenfell, R. Hein, D. Shindell, and J. Staehelin (2001), Origin and variability of upper tropospheric nitrogen oxides and ozone at northern mid-latitudes, *Atmos. Environ.*, *35*, 3421–3433, doi:10.1016/S1352-2310(01)00134-0.

Jacobson, M. Z., and D. G. Streets (2009), Influence of future anthropogenic emissions on climate, natural emissions, and air quality, *J. Geophys. Res.*, *114*, D08,118, doi:10.1029/2008JD011476.

Jiang, H., and H. Liao (2013), Projected changes in NOx emissions from lightning as a result of 2000-2050 climate change, *Atmos. Oceanic Sci. Lett.*, *6*(5), 284–289, doi:

10.3878/j.issn.1674-2834.13.0042.1.

Johnson, P. C. (2014), Extension of Nakagawa & Schielzeth's R2 GLMM to random slopes models, *Methods Ecol. Evol.*, *5*, 944–946, doi:10.1111/2041-210X.12225.

Jourdain, L., and D. A. Hauglustaine (2001), The global distribution of lightning NOx eimulated on-line in a general circulation model, *Phys. Chem. Earth Pt C*, *26*(8), 585–591.

Lamarque, J.-F., D. T. Shindell, B. Josse, P. J. Young, I. Cionni, V. Eyring, D. Bergmann, P. Cameron-Smith, W. J. Collins, R. Doherty, S. Dalsoren, G. Faluvegi, G. Folberth, S. J. Ghan, L. W. Horowitz, Y. H. Lee, I. A. MacKenzie, T. Nagashima, V. Naik, D. Plummer, M. Righi, S. T. Rumbold, M. Schulz, R. B. Skeie, D. S. Stevenson, S. Strode, K. Sudo, S. Szopa, A. Voulgarakis, and G. Zeng (2013), The Atmospheric Chemistry and Climate Model Intercomparison Project (ACCMIP): Overview and description of models, simulations and climate diagnostics, *Geosci. Model Dev.*, *6*(1), 179–206, doi:10.5194/gmd-6-179-2013.

Liaskos, C. E., D. J. Allen, and K. E. Pickering (2015), Sensitivity of tropical tropospheric composition to lightning NOx production as determined by the NASA GEOS-Replay model, *J. Geophys. Res. Atmos.*, *120*, 8512–8534, doi:10.1002/2014JD022987.

Meijer, E., P. van Velthoven, D. Brunner, H. Huntrieser, and H. Kelder (2001), Improvement and evaluation of the parameterisation of nitrogen oxide production by lightning, *Phys. Chem. Earth Pt C*, *26*(8), 577–583, doi:10.1016/S1464-1917(01)00050-2.

Nakagawa, S., and H. Schielzeth (2013), A general and simple method for obtaining R2 from generalized linear mixed-effects models, *Methods Ecol. Evol.*, *4*(2), 133–142, doi:

10.1111/j.2041-210x.2012.00261.x.

Ott, L. E., K. E. Pickering, G. L. Stenchikov, D. J. Allen, A. J. DeCaria, B. Ridley, R.-F. Lin, S. Lang, and W.-K. Tao (2010), Production of lightning NOx and its vertical distribution calculated from three-dimensional cloud-scale chemical transport model simulations, *J. Geophys. Res.*, *115*, D04,301, doi:10.1029/2009JD011880.

Pickering, K. E., Y. Wang, W.-K. Tao, C. Price, and J.-F. Muller (1998), Vertical distributions of lightning NOx for use in regional and global chemical transport models, *J. Geophys. Res.*, *103*(D23), 31,203–31,216.

Pinheiro, J. C., and D. M. Bates (2000), *Mixed-Effects Models in S and S-PLUS*, Springer.

Price, C., and D. Rind (1992), A simple lightning parameterization for calculating global lightning distributions, *J. Geophys. Res.*, *97*(D9), 9919–9933, doi:10.1029/92JD00719.

Price, C., and D. Rind (1994), Possible implications of global climate change on global lightning distributions and frequencies, *J. Geophys. Res.*, *99*(94), 10,823–10,831.

Price, C., J. Penner, and M. Prather (1997), NOx from lightning 1. Global distribution based on lightning physics, *J. Geophys. Res.*, *102*(D5), 5929–5941.

Reynolds, S. E., M. Brook, and M. F. Gourley (1957), Thunderstorm charge separation, *J. Meteorol.*, *14*, 426–436.

Romps, D. M. (2014), Projected increase in lightning strikes in the United States due to global warming, *Science*, *346*(6211), doi:10.1126/science.1259100.

Schumann, U., and H. Huntrieser (2007), The global lightning-induced nitrogen oxides source, *Atmos. Chem. Phys.*, *7*, 3823–3907, doi:10.5194/acpd-7-2623-2007.

Stevenson, D., R. Doherty, M. Sanderson, C. Johnson, B. Collins, and D. Derwent (2005), Impacts of climate change and variability on tropospheric ozone and its precursors, *Faraday Discuss.*, *130*, 41, doi:10.1039/b417412g.

Stockwell, D. Z., C. Giannakopoulos, P. H. Plantevin, G. D. Carver, M. P. Chipperfield, K. S. Law, J. A. Pyle, D. E. Shallcross, and K. Y. Wang (1999), Modelling NOx from lightning and its impact on global chemical fields, *Atmos. Environ.*, *33*, 4477–4493, doi:10.1016/S1352-2310(99)00190-9.

Tost, H., P. Jöckel, and J. Lelieveld (2007), Lightning and convection parameterisations - uncertainties in global modelling, *Atmos. Chem. Phys.*, *7*(3), 4553–4568, doi:10.5194/acpd-7-6767-2007.

Wild, O. (2007), Modelling the global tropospheric ozone budget: Exploring the variability in current models, *Atmos. Chem. Phys.*, *7*, 2643–2660, doi:10.5194/acp-7-2643-2007.

Williams, E. (2005), Lightning and climate: A review, *Atmos. Res.*, *76*(1-4), 272–287, doi:10.1016/j.atmosres.2004.11.014.

Wong, J., M. C. Barth, and D. Noone (2013), Evaluating a lightning parameterization based on cloud-top height for mesoscale numerical model simulations, *Geosci. Model Dev.*, *6*, 429–443, doi:10.5194/gmd-6-429-2013.

Wu, S., L. J. Mickley, D. J. Jacob, J. A. Logan, R. M. Yantosca, and D. Rind (2007), Why are there large differences between models in global budgets of tropospheric ozone?, *J. Geophys. Res.*, *112*, D05,302, doi:10.1029/2006JD007801.

Yoshida, S., T. Morimoto, T. Ushio, and Z. Kawasaki (2009), A fifth-power relationship for lightning activity from Tropical Rainfall Measuring Mission satellite observations,

J. Geophys. Res., *114*, D09,104, doi:10.1029/2008JD010370.

Young, P. J., A. T. Archibald, K. W. Bowman, J.-F. Lamarque, V. Naik, D. S. Stevenson, S. Tilmes, A. Voulgarakis, O. Wild, D. Bergmann, P. Cameron-Smith, I. Cionni, W. J. Collins, S. B. Dalsøren, R. M. Doherty, V. Eyring, G. Faluvegi, L. W. Horowitz, B. Josse, Y. H. Lee, I. A. MacKenzie, T. Nagashima, D. A. Plummer, M. Righi, S. T. Rumbold, R. B. Skeie, D. T. Shindell, S. A. Strode, K. Sudo, S. Szopa, and G. Zeng (2013), Pre-industrial to end 21st century projections of tropospheric ozone from the Atmospheric Chemistry and Climate Model Intercomparison Project (ACCMIP), *Atmos. Chem. Phys.*, *13*, 2063–2090, doi:10.5194/acp-13-2063-2013.

Zeng, G., J. A. Pyle, and P. J. Young (2008), Impact of climate change on tropospheric ozone and its global budgets, *Atmos. Chem. Phys.*, *8*(2), 369–387, doi:10.5194/acp-8-369-2008.

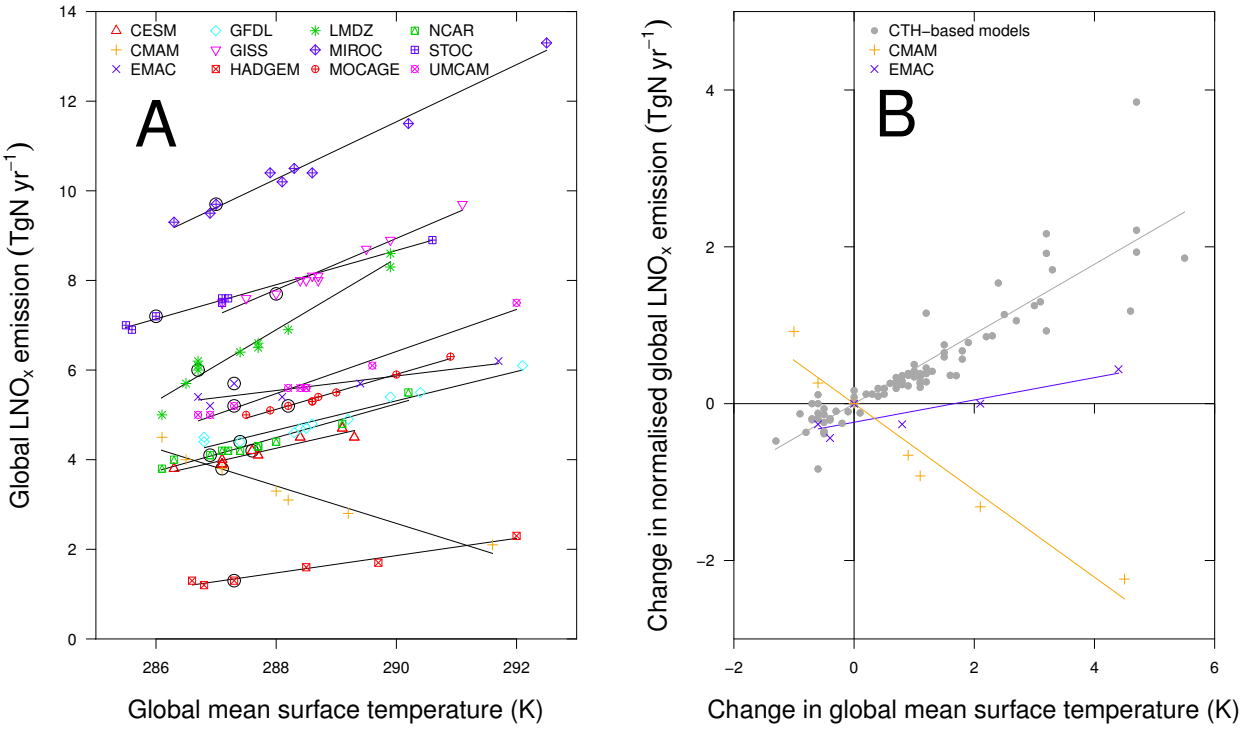

Figure 1. Total annual lightning NO_x emissions against global mean surface temperature for the ACCMIP models with interactive lightning schemes. Absolute global emissions and surface temperatures are shown in panel (A); changes in lightning NO_x emissions with respect to the year 2000 baseline, normalised to 5 TgN in year 2000, and grouped according to lightning parametrization are shown in panel (B). Circled points in A are from the year 2000 baseline simulations.

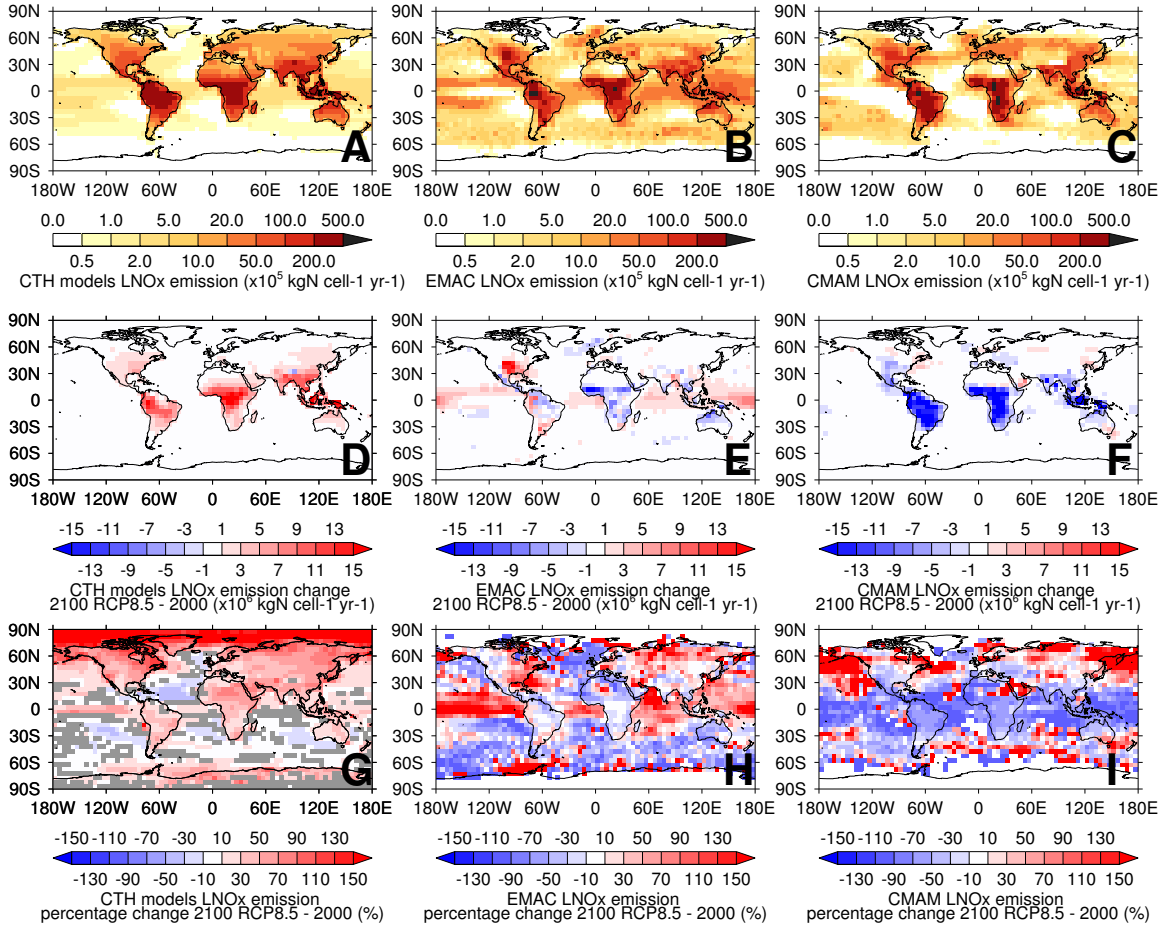

Figure 2. Annual vertically-integrated lightning NO_x emission distribution for the year 2000 baseline and absolute and percentage change with respect to RCP8.5 year 2100. Annual emissions for year 2000 baseline are normalised to 5 TgN for all models with the same normalisation factors applied to year 2100 RCP8.5 emissions. The top row shows the baseline distributions for year 2000, the second row shows the absolute changes in distribution for the year 2100 RCP8.5 experiments, and the bottom row shows the equivalent percentage changes. The left column panels are the mean of eight models using the cloud-top height approach. The middle and right columns plots are the individual results for the EMAC and CMAM models, respectively. Mean values are calculated after scaling and regridding all models to a common resolution (5° x 5°). In (G) the greyed cells represent grid cells in which there is not at least five models that estimate the same sign of change.

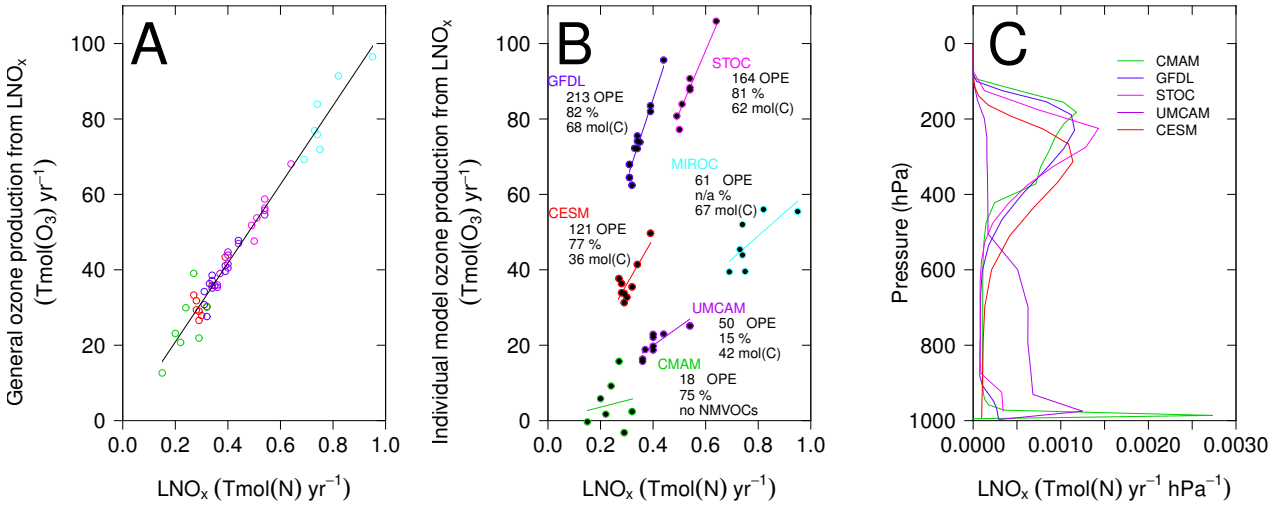

Figure 3. Tropospheric ozone production from lightning NO_x emissions and the role of NMVOC emissions and the vertical distribution of lightning NO_x emissions. A) "General ozone production from LNO_x" is a partial residual with respect to LNO_x described by Equation 2. B) "Individual model ozone production from LNO_x" is a partial residual with respect to LNO_x described by Equation 3. The text in B) for each model is, from top to bottom, the ozone production efficiency (OPE) from LNO_x, the percentage of baseline lightning NO_x emissions in the middle and upper troposphere [500-100 hPa], and the mean NMVOC emissions. C) is the baseline global LNO_x vertical distribution. The MIROC model is not included in (C) because the emission distribution was not archived. For (C), values of pressure are based on a uniform 1000 hPa surface pressure and annual lightning NO_x emissions are normalised to 5 TgN.